FEBS openbio

FEBS PRESS science publishing by scientists

PKU mutation p.G46S prevents the stereospecific binding of L-phenylalanine to the dimer of human phenylalanine hydroxylase regulatory domain

João Leandro[1,2], Jaakko Saraste[1], Paula Leandro[2] and Torgeir Flatmark[1]

1 Department of Biomedicine, University of Bergen, Norway
2 Metabolism and Genetics Group, Research Institute for Medicines and Pharmaceutical Sciences (iMed.UL), Faculty of Pharmacy, University of Lisbon, Portugal

Keywords
βαββαβ folds; phenylalanine hydroxylase; regulatory domain

Correspondence
T. Flatmark, Department of Biomedicine, University of Bergen, Jonas Lies vei 91, N-5009 Bergen, Norway
Fax: +47 55586360
Tel: +47 55586428
E-mail: torgeir.flatmark@biomed.uib.no

(Received 10 November 2016, revised 1 December 2016, accepted 3 December 2016)

doi:10.1002/2211-5463.12175

Mammalian phenylalanine hydroxylase (PAH) has a potential allosteric regulatory binding site for L-phenylalanine (L-Phe), in addition to its catalytic site. This arrangement is supported by a crystal structure of a homodimeric truncated form of the regulatory domain of human PAH (hPAH-RD$^{1–118/19–118}$) [Patel D *et al.* (2016) *Sci Rep* doi: 10.1038/srep23748]. In this study, a fusion protein of the domain (MBP-(pep$_{Xa}$)-hPAH-RD$^{1–120}$) was overexpressed and recovered in a metastable and soluble state, which allowed the isolation of a dimeric and a monomeric fusion protein. When cleaved from MBP, hPAH-RD forms aggregates which are stereospecifically inhibited by L-Phe (> 95%) at low physiological concentrations. Aggregation of the cleaved dimer of the mutant form hPAH-G46S-RD was not inhibited by L-Phe, which is compatible with structurally/conformationally changed βαβϖ βαβ ACT domain folds in the mutant.

Enzyme kinetic and biophysical studies of the full-length rat and human phenylalanine hydroxylase (r/hPAH) homotetramer have indicated that its catalytic activation by L-phenylalanine (L-Phe) involves a slow (*s*-to-*min* timescale) global conformational change, preceding the chemical steps characteristic of a hysteretic enzyme [1,2]. Mammalian PAH shows a complex activation mechanism. Based on indirect experimental evidence, two main working models have been proposed: (i) binding of L-Phe to a putative allosteric site in the N-terminal regulatory domain (RD) as well as to the catalytic site [3–8], and (ii) cooperative binding of L-Phe (n_H about 2) at the catalytic site which represents the site of initiation ('epicentre') for the conformational transition in the activation process [9–14]. The first model was originally based on indirect enzyme kinetic and biophysical studies on the rPAH tetramer and truncated RD constructs, but has lately gained further support from the determination of the X-ray crystal structure of the full-length ligand-free and autoinhibited rat and human enzyme at low resolution (PDB ID: 5DEN at 2.9 Å [15] and PDB ID: 5EGQ at 3.6 Å) [8]) and the high resolution crystal structure (PDB ID: 5FII at 1.8 Å) of a homodimeric truncated form of the human RD (hPAH-RD) [16]. Representing the key finding of this study, the structure revealed two L-Phe molecules bound to a homodimer at the interphase of the two $\beta_1\alpha_1\beta_2\beta_3\alpha_2\beta_4$ ACT domain folds along the plane of the twofold axis [16]. However, in the absence of L-Phe, the overexpressed construct aggregated.

The missense mutation p.G46S in hPAH (Fig. 1) is associated with a severe form of phenylketonuria and

Abbreviations
ANS, 8-anilino-1-naphthalenesulfonic acid; MBP, maltose-binding protein; n_H, Hill coefficient; PAH, phenylalanine hydroxylase; RD, regulatory domain; SAXS, small angle X-ray scattering; SEC, size-exclusion chromatography.

generates a misfolded protein which is rapidly degraded on expression in HEK293 cells [17]. The crystal structure of the wt-hPAH-RD has shown that L-Phe binding includes the sequence region E^{43}xVxAL in the two protomers [16], and it was therefore of great interest to test the effect of a G→S substitution on the L-Phe binding to the $\beta_1\alpha_1\beta_2\beta_3\alpha_2\beta_4$ ACT domain folds in the hPAH-G46S-RD mutant form. Since a previous attempt has failed to express this mutant form in a nonaggregated and soluble form [16], we here overexpressed it as a fusion protein (MBP-$(pep)_{Xa}$-hPAH-RD). This change in the RD construct results in a stabilization of both the wt and mutant forms of the RD protein in a metastable and soluble state, and allows the isolation of a dimeric and a monomeric fusion protein. When cleaved by factor Xa, the maltose-binding protein (MBP)-free wt-RD of both forms undergoes aggregation, which is stereospecifically prevented by L-Phe. Thus, the substrate stabilizes a dimer of the RD. 8-Anilino-1-naphthalenesulfonic acid (ANS) binding studies with the dimeric wt fusion protein confirmed the stereospecific binding of L-Phe in a physiological concentration range. With reference to the behaviour of the wt-hPAH-RD, it is shown that L-Phe does not bind and stabilize the mutant form hPAH-G46S-RD due to a structural/conformational change in its wt-binding site involving residues E^{43}xVxAL in the dimeric $\beta_1\alpha_1\beta_2\beta_3\alpha_2\beta_4$ ACT domain folds.

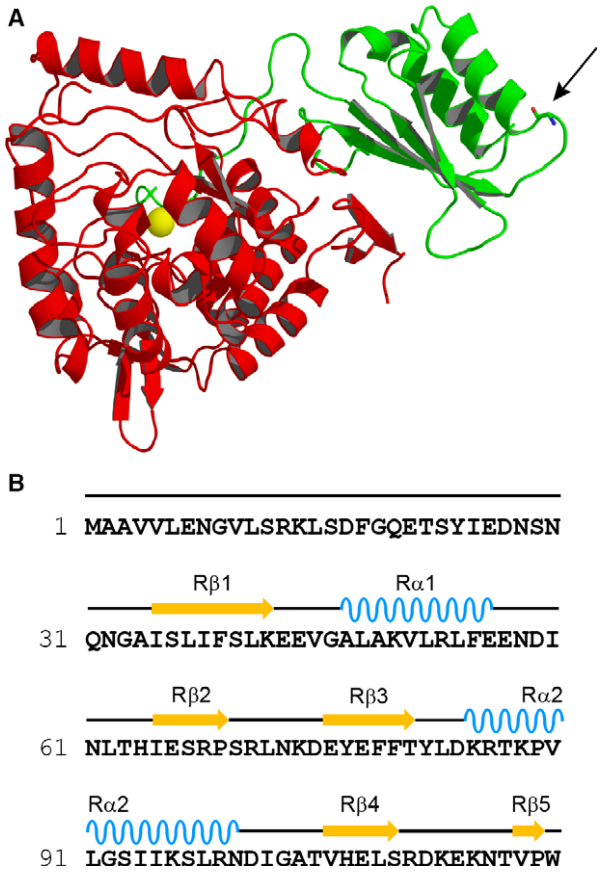

Fig. 1. 3D structure of PAH protomer ($rPAH^{1–429}$), sequence and secondary structure assignment of the N-terminal regulatory domain (RD) of hPAH and the localization/interactions of the G46 residue in the RD. (A) Ribbon representation of the regulatory/catalytic domain crystal structure of rPAH (PDB ID: 1PHZ at the highest resolution (2.2 Å) for this structure) in the monomeric form with the RD shown in green, the catalytic domain in red, the iron as a yellow sphere and G46 in stick model (pointed arrow). (B) Sequence of the N-terminal regulatory domain of hPAH (SwissProt P00439) with elements of secondary structure (determined from the coordinates of PDB ID: 1PHZ with the program DSSP [26] indicated above the sequence and numbered sequentially from the N terminus [4]. Figure (A) was created using PyMOL, version 1.1 (DeLano Scientific) [27].

Materials and methods

TB1 cells, the prokaryotic expression vector pMAL-c2/pMAL-hPAH and the amylose resin were obtained from New England Biolabs (Ipswich, MA, USA). The restriction protease factor Xa was obtained from Protein Engineering Technology ApS (Aarhus, Denmark). ANS were obtained from Sigma-Aldrich (Oslo, Norway).

Site-specific mutagenesis

The wt-RD (pMAL-hPAH-$RD^{1–120}$) and its G46S mutant form (pMAL-hPAH-G46S-$RD^{1–120}$) were obtained by introducing a stop signal in codon 121 of hPAH by site-directed mutagenesis (QuikChange® II; Stratagene, Santa Clara, CA, USA), using the wt-pMAL-hPAH [18] and pMAL-G46S-hPAH constructs [17] as templates respectively. Primers 5′-GACACAGTGCCCTGGT**AA**CCAA GAACCATTCAAGAGC-3′ (forward) and 5′-GCTCTTG AATGGTTCTTGG**TT**ACCAGGGCACTGTGTC-3′ (reverse) used for mutagenesis were provided by Eurogentec (Seraing, Belgium; the mismatch nucleotides are shown in bold). The authenticity of the mutagenesis was verified by DNA sequencing as described previously [17].

Overexpression and isolation of fusion proteins

The wt and G46S mutant forms of hPAH-RD were overexpressed in *Escherichia coli* as fusion proteins (MBP-$(pep)_{Xa}$-hPAH-RD) [18]. The bacteria were grown at 37 °C and the induction by 1 mM isopropyl-thio-β-D-galactoside was performed for 8 h at 28 °C. The fusion proteins were purified by affinity chromatography (amylose resin) and centrifuged in a TL-100 Ultracentrifuge (Beckman, Indianapolis, IN, USA) for 20 min at 50 000 ***g*** before size-exclusion chromatography (SEC), as described earlier [18]. SEC was performed as described in the legend to Fig. 2. The

dimeric and monomeric protein fractions were concentrated by Centriplus 30 filter (Amicon, Darmstadt, Germany). The concentration of purified fusion proteins was measured using the absorption coefficient A_{280} (1 mg·mL^{-1}·cm^{-1}) = 1.34. A colorimetric method [19] was in some cases also used to measure enzyme concentrations, with bovine serum albumin as the standard.

Cleavage of MBP-hPAH-RD fusion proteins and assay of self-association by light scattering

Before cleavage of the MBP-hPAH-RD fusion proteins by factor Xa they were centrifuged at 210 000 ***g*** for 15 min at 4 °C. In the standard assay at 20 mM Na-Hepes, 0.1 M NaCl, pH 7.0 and 25 °C the concentration of the fusion protein was 0.74 mg·mL^{-1}, and the concentration of factor Xa was adjusted to give a final ratio (by weight) of 1 : 150 relative to the fusion protein. Self-association (aggregation) of the factor Xa-released RD was followed in real-time by light scattering, as measured by the increase in the apparent absorbance at 350 nm $A'_{350} = \log [I_o/(I_p + fI_d)]$, using an Agilent 8453 Diode Array Spectrophotometer (Matriks AS, Oslo, Norway) with a Peltier temperature control unit as previously described [20]. The change in light scattering was expressed as $\Delta A'_{350}$ by subtracting the background absorbance in the absence of the added factor Xa. The rate of oligomerization was expressed as $\Delta A'_{350}/\Delta t$ and was obtained from the slope of the linear growth phase of each light scattering curve. In each experiment a parallel time-course cleavage analysis was conducted to rule out any effect of the cleavage rate.

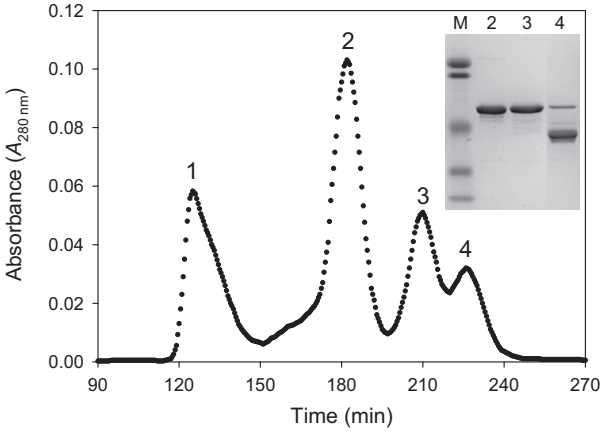

Fig. 2. Size-exclusion chromatography of the MBP-hPAH-RD$^{1–120}$ construct. Peak 1, higher order oligomeric forms (eluted at the void volume); peak 2, dimeric form (~ 156 kDa); peak 3, monomeric form (~ 65 kDa), and peak 4, degradation products (~ 39 kDa). The molecular mass of the enzyme forms were estimated using the elution position of standard molecular mass markers as a reference (not shown). 10.7 mg of fusion protein were applied to the column. The chromatography was performed on a HiLoad Superdex 200 HR column (1.6 cm × 60 cm) from Amersham Biosciences (GE Healthcare, Oslo, Norway), equilibrated and eluted with 20 mM Na-Hepes, 0.2 M NaCl, pH 7.0 at a flow rate of 0.38 mL·min^{-1} at 4 °C and detection was at 280 nm. The inset represents a SDS/PAGE analysis demonstrating the purity of the fusion proteins after two steps of purification. Lane M, low molecular mass standard (106.5, 97.6, 50.2, 36.9 and 28.9 kDa); lane 2, dimeric form (peak 2); lane 3, monomeric form (peak 3) and lane 4, degradation products (peak 4) after the size-exclusion chromatography.

In order to study the inhibitory effect of L-Phe/D-Phe on aggregation of MBP-free wt-hPAH-RD and its mutant form, the fusion proteins were preincubated for 5 min at standard assay conditions with L-Phe (0–1 mM) before the cleavage was initiated with factor Xa. The inhibition of aggregation was analysed by the SigmaPlot® Technical Graphing Software (Alfasoft AS, Lillestrøm, Norway). The Hill plot analyses for the inhibition was performed as previously described [21], and the Hill coefficient (n_H) was calculated by fitting the data into the linear form of the Hill plot equation: $\log[v_i/(v_o - v_i)] = n_H \log[L] - n_H \log[k]$. $[L]_{0.5}$ represents the concentration of L-Phe at 50% inhibition.

SDS/PAGE analyses

The purification of the fusion proteins and the efficiency of its cleavage by factor Xa, was analysed by SDS/PAGE in a 10% (w/v) polyacrylamide gel [22]. The gels were stained by Coomassie Brilliant Blue R-250, scanned using Versa-Doc 4000 (Bio-Rad, Hercules, CA, USA) and quantification of the protein bands was carried out by using the Quantity One 1-D Analysis Software (Bio-Rad).

ANS-binding assay

Fluorescence-based ANS binding studies were performed as described [23]. The fluorescence emission spectra were recorded between 400 and 600 nm (6-nm slit width) at 25 °C using an excitation wavelength of 385 nm (6-nm slit width) on a Perkin-Elmer LS-50B luminescence spectrometer (Perkin-Elmer, Waltham, MA, USA) and by averaging four scans.

Negative staining of wt-hPAH-RD oligomers and electron microscopy

For negative staining EM of wt-hPAH-RD oligomers, Formvar-coated 200 mesh nickel grids (Electron Microscopy Sciences, Hatfield, PA, USA) were used. The grids were further coated with carbon, stored dust-free in Petri dishes kept at low humidity and glow-discharged for 15 s prior to use. Negative staining was carried out by first applying 5 μL of a protein solution on the specimen grid. Following absorption for 60 s, the sample drop was removed by blotting with filter paper, and the grid was stained twice with 2% (w/v) aqueous uranyl acetate. After application, the first drop of stain (10 μL) was blotted off immediately,

whereafter a fresh drop of the stain was added to the grid for 15 s. After final blotting and drying, the specimens were observed in a Jeol 1230 Electron Microscope (Jeol USA, Inc., Peabody, MA, USA) operated at 80 kV.

Results

Overexpression and isolation of the wt-MBP-hPAH-RD fusion proteins

On overexpression of wt-MBP-$(pep)_{Xa}$-hPAH-$RD^{1–120}$ the soluble affinity purified fusion protein was separated by SEC into oligomeric forms and some aggregates. The chromatogram of the fusion protein (10.7 mg; Fig. 2) revealed four peaks, where peak 1 represented minor aggregates eluted at or near the void volume, while peak 2 and peak 3 represented the dimeric and monomeric forms respectively. Identical mobilities were observed for peaks 2 and 3 on SDS/PAGE (Fig. 2), with an apparent molecular mass of ~ 63 kDa. Peak 4 represents degradation products.

Cleavage of the MBP stabilized wt fusion proteins

At the standard assay conditions (pH 7.0, 0.1 M NaCl and 25 °C) the cleavage of the metastable and soluble wt-MBP-hPAH-RD fusion proteins (~ 0.7 $mg{\cdot}mL^{-1}$) by factor Xa (5.0 $\mu g{\cdot}mL^{-1}$) was very similar for the dimeric and the monomeric fusion protein, with $t_{1/2}$ (time at 50% cleavage) of ~ 11 min. The presence of L-Phe had no significant effect on the cleavage of wt-MBP-hPAH-RD by factor Xa.

Aggregation of wt-hPAH-RD upon cleavage of dimeric and monomeric MBP fusion proteins and its stereospecific inhibition by L-Phe

On cleavage of equal amounts (~ 0.7 $mg{\cdot}mL^{-1}$) the dimeric and monomeric MBP-hPAH-RD fusion proteins by factor X_a (5.0 $\mu g{\cdot}mL^{-1}$) aggregates are formed (Fig. 3), with a similar time-course observed for the two fractions. It includes a delay period (lag phase), and a growth phase of increasing light scattering $(\Delta A'_{350}/\Delta t)_{max}$ of $3.9 \pm 0.1 \times 10^{-3}$ and $1.3 \pm 0.1 \times 10^{-3}$ $AU{\cdot}min^{-1}$, for the dimeric (Fig. 3A) and monomeric (Fig. 3B) protein fractions respectively. For ultrastructure of the aggregates and soluble protein (see Fig. 7 below). In the absence of added factor Xa no change in light scattering was observed for the two fractions within the time frame of 3 h.

The aggregation of the MBP-free RD is inhibited in a stereospecific manner by L-Phe; 100 μM L-Phe almost completely protects against the aggregation, whereas 100 μM D-Phe and other L-amino acids gave no effect (Fig. 4A). The inhibition revealed a $[L]_{0.5}$ value of 23.3 ± 0.5 μM L-Phe on cleavage of the dimeric form, with a positive cooperativity; the Hill coefficient was calculated to be about 2 ($n_H = 2.05$) (see Materials and methods section). A similar stereospecificity was observed on factor Xa cleavage of the monomeric

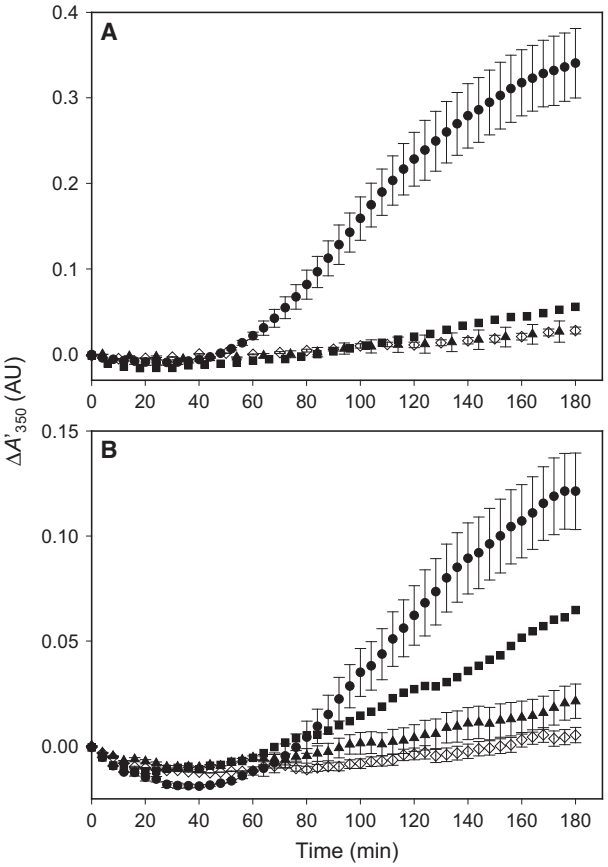

Fig. 3. The self-association of $hPAH\text{-}RD^{1–120}$ following cleavage of dimeric (A) and monomeric (B) MBP fusion proteins by factor Xa, and the effect of L-Phe. (A) The time-course of the self-association was followed in real-time by light scattering, as measured by the increase in the apparent absorbance at 350 nm ($\Delta A'_{350}$). The data points correspond to dimeric wt-$hPAH^{1–120}$ fusion protein following cleavage by factor Xa in the absence of any added compound (●) and in the presence of 1 mM L-Phe (▲). (◊) represents dimeric wt-$hPAH^{1–120}$ fusion protein in the absence of factor Xa. (B) The time-course of the self-association in the absence of any added compound (●) and in the presence of 1 mM L-Phe (▲). (◊) represents monomeric wt-$hPAH^{1–120}$ fusion protein in the absence of factor Xa. The reactions were performed at standard assay conditions (0.74 $mg{\cdot}mL^{-1}$ fusion protein, 5.0 $\mu g{\cdot}mL^{-1}$ factor Xa, 20 mM Na-Hepes, 0.1 M NaCl, pH 7.0 and 25 °C). Some data points were omitted for clarity. Error bars represent mean ± SD ($n = 3$).

fraction (data not shown), and the $[L]_{0.5}$ value for the inhibition of aggregation was 15.1 ± 2.4 μM L-Phe, but with a hyperbolic inhibition curve (Fig. 5B).

Binding of ANS to wt-MBP-hPAH-RD before and after cleavage

8-Anilino-1-naphthalenesulfonic acid is a spectroscopic probe displaying affinity for hydrophobic clusters which are not tightly packed in a fully folded structure, or become exposed in partially unfolded structures [24]. ANS binds to ligand-free dimeric wt-MBP-hPAH-RD fusion protein (Fig. 6A), and its factor Xa cleaved forms (t = 3 h) (Fig. 6B), with an increase in the fluorescence intensity and a blue shift (maximum at ~ 478 nm), resulting from the binding. Identical spectra were obtained in the absence and presence of 1 mM D-Phe, whereas L-Phe revealed a concentration-dependent decrease, in a physiological concentration range, and a red shift of the fluorescence spectra (Fig. 6A,B). A much smaller effect of L-Phe on

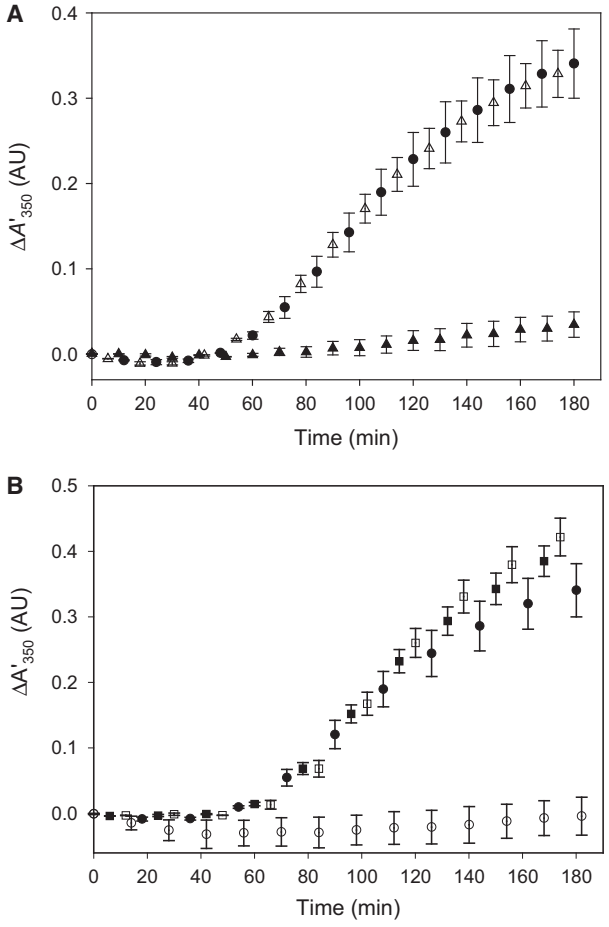

Fig. 4. (A) The stereospecific inhibition of the self-association of hPAH-RD$^{1–120}$ by phenylalanine. The time-course of the self-association of hPAH-RD$^{1–120}$ protein following cleavage of themdimeric fusion protein by factor Xa in the absence (●) and presence of 100 μM L-Phe (▲) or 100 μM D-Phe (△). (B) The self-association of dimeric hPAH-RD$^{1–120}$ and its G46S mutant form and the effect of L-Phe. The time-course of the self-association of hPAH-RD$^{1–120}$ dimeric protein following cleavage of the fusion protein by factor Xa in the absence (●) and presence of 150 μM L-Phe (○); hPAH-G46S-RD$^{1–120}$ dimer fusion protein following cleavage by factor Xa in the absence (■) and presence of 150 μM L-Phe (□). Some data points were omitted for clarity. The assays were performed at standard assay conditions and error bars represent mean ± SD, n = 3 independent experiments.

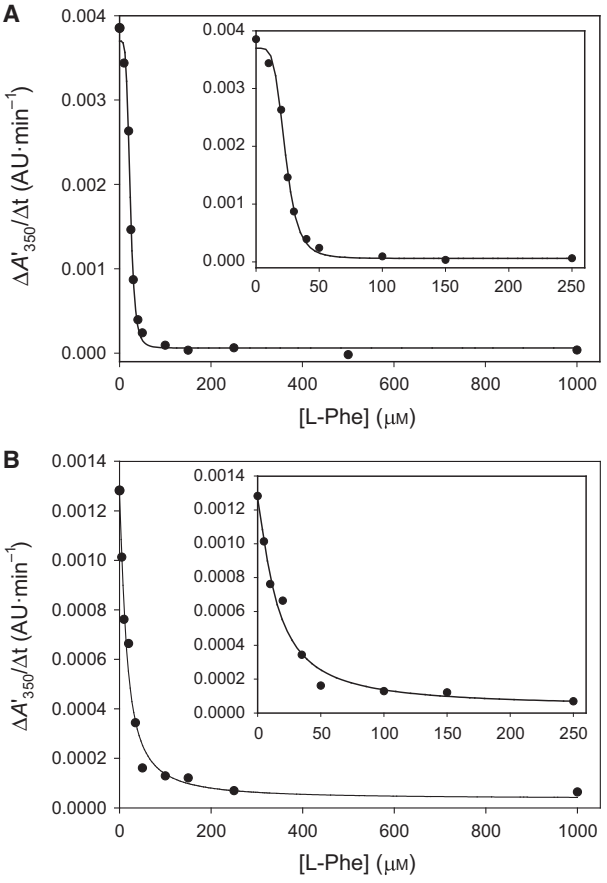

Fig. 5. The effect of L-Phe concentration on the inhibition of the self-association (aggregation) of dimeric (A) and monomeric (B) MBP fusion protein hPAH-RD$^{1–120}$. The inhibitory effect of L-Phe on the aggregation was assayed at standard conditions (0.74 mg·mL^{-1} fusion protein, 5.0 μg·mL^{-1} factor Xa, 20 mM Na-Hepes, 0.1 M NaCl, pH 7.0 and 25 °C) with varying concentrations of L-Phe (0–1 mM) and the rate of forming higher order oligomers ($\Delta A'_{350}/\Delta t$) was obtained from the slope of the linear growth phase of each light scattering curve. The L-Phe dose-dependent inhibition curves of the aggregation were generated by nonlinear regression analysis of the experimental data using the four parameter logistic equation (see Materials and methods). The insets represent the data obtained at the concentration range 0–250 μM L-Phe.

ANS binding was observed for the monomeric fusion protein fraction (Fig. 6C,D), which is slightly contaminated by the dimeric form, due to its chromatograpgic tailing. The MBP fusion partner alone has a negligible contribution to the ANS fluorescence, and there was no additional effect of L-Phe (Fig. 6A).

L-Phe does not protect against aggregation of the hPAH-G46S-RD mutant form

When the mutant protein hPAH-G46S-RD is overexpressed in *E. coli*, mainly insoluble protein is recovered [17]. In contrast, here the fusion protein MBP-hPAH-G46S-RD was isolated as a metastable and soluble protein (Fig. 4B). On SEC chromatography only the dimeric form was recovered at sufficiently high yield for further analyses (Fig. 4B), and it revealed the same electrophoretic mobility on SDS/PAGE as the wt dimeric RD. In the absence of added factor Xa no change in light scattering was observed within 3 h. Upon cleavage by factor Xa, the MBP-free G46S-RD aggregated, but in this case no protection against aggregation by L-Phe was observed (Fig. 4B) at concentrations up to 1 mM

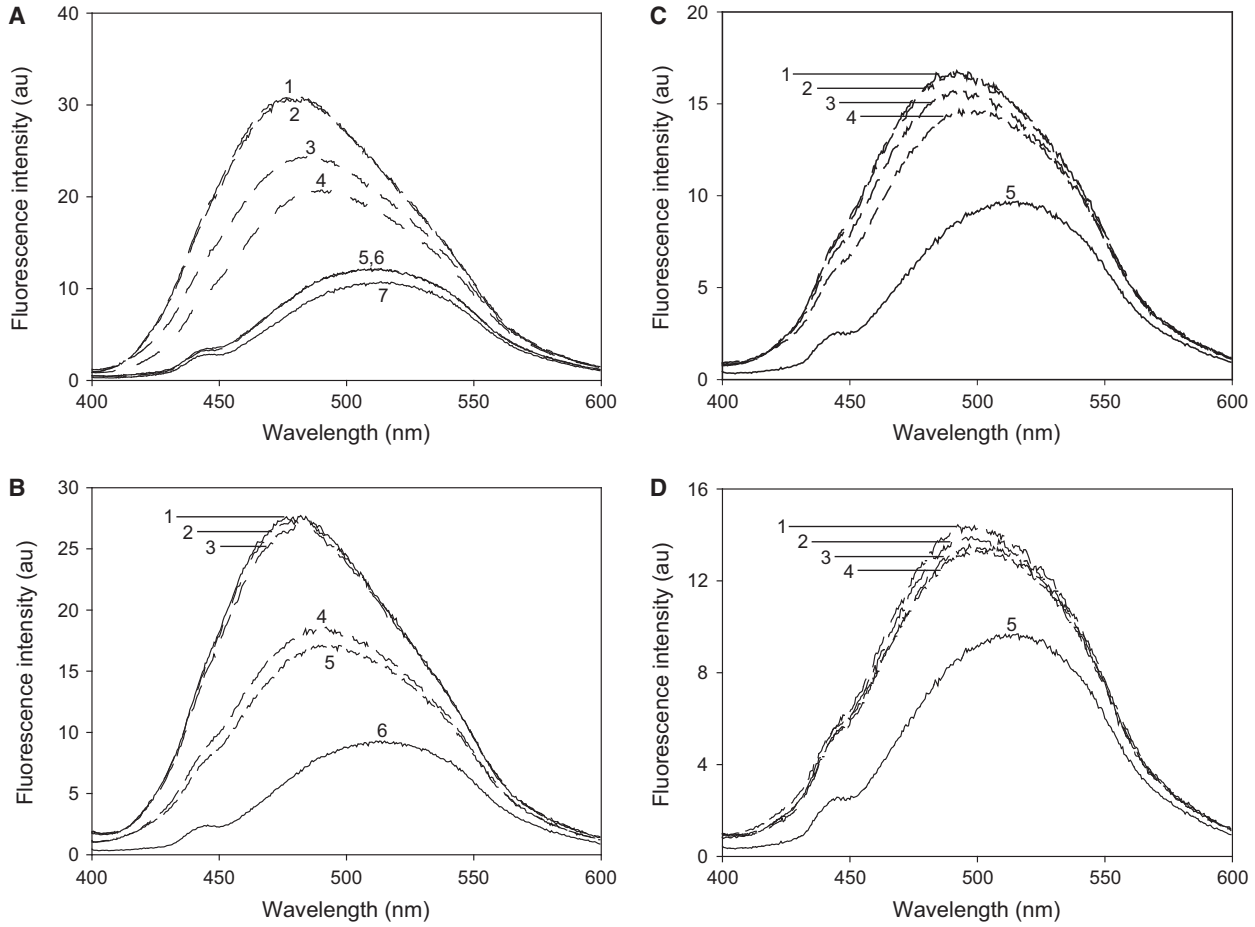

Fig. 6. The binding of ANS to dimeric fusion protein MBP-hPAH-RD$^{1–120}$. Briefly, 1.3 μM MBP-hPAH-RD was incubated with 60 μM ANS in 20 mM Na-Hepes, 0.1 M NaCl, pH 7.0 at room temperature for 5 min in the dark. (A) ANS fluorescence emission spectra of the fusion protein in the absence of ligand (trace 1), with 100 μM L-Phe (*trace* 3), 1 mM L-Phe (trace 4), and 1 mM D-Phe (*trace* 2). The MBP protein was used as a control in the absence (trace 5) and in the presence of 1 mM L-Phe (trace 6) and the emission spectrum of buffer with ANS is shown (trace 7). (B) ANS fluorescence emission spectra observed after cleavage of the dimeric MBP-hPAH-RD$^{1–120}$ fusion protein by factor Xa (t = 3 h) in the absence of ligand (trace 1), with 100 μM L-Phe (trace 4), 1 mM L-Phe (trace 5), 100 μM D-Phe (trace 2), 1 mM D-Phe (trace 3) and the emission spectrum of buffer with ANS (trace 6). (C) ANS fluorescence emission spectra of the monomeric wt-hPAH$^{1–120}$ fusion protein in the absence of ligand (trace 1), with 100 μM L-Phe (trace 3), 1 mM L-Phe (trace 4), 1 mM D-Phe (trace 2) and the emission spectrum of buffer with ANS (trace 5). (D) ANS fluorescence emission spectra observed after cleavage of the monomeric wt-hPAH$^{1–120}$ fusion protein by factor Xa (t = 3 h) in the absence of ligand (trace 1), with 100 μM L-Phe (trace 3), 1 mM L-Phe (*trace* 4), 1 mM D-Phe (trace 2) and the emission spectrum of buffer with ANS (trace 5). The excitation wavelength was 385 nm.

that inhibited wt-RD dimer aggregation by > 95% (Fig. 5A).

Ultrastructure of wt-hPAH-RD oligomers

In order to get information on the fine structure of the wt-hPAH-RD$^{1–120}$ protein and its higher order aggregates that are both formed on factor Xa cleavage of the fusion protein, negative staining EM was performed on aliquots removed at different times during the cleavage reaction. EM micrographs corresponding to the final time point (t = 180 min) with complete cleavage (Fig. 7) revealed that while the self-association of the wt protein generated some unstructured higher order aggregates, the main field is dominated by small structures with a dimeric appearance.

Discussion

A recent SAXS analysis of the rat PAH homotetramer lead to the proposal that the L-Phe-induced activation and associated conformational changes involve dimerization of the RDs, creating two binding sites for L-Phe [8]. These binding sites have later been defined in a high resolution (1.8 Å) structure of a homodimeric truncated form of hPAH-RD in complex with L-Phe [16]. In the same study on size-exclusion chromatography of hPAH-RD$^{1–118}$ and hPAH-RD$^{19–118}$, both constructs are reported to elute as a mixed population of monomer and higher order aggregates. However, the addition of L-Phe stabilizes the constructs and reduces their aggregation tendency, likely through domain dimerization [16]. In the present study, it is found that expressing a similar construct of the human RD as a MBP fusion protein (MBP-hPAH-RD) preserves the recombinant protein in a metastable conformational state, which protects against aggregation since MBP functions as a molecular chaperone [25]. The dimeric and monomeric fractions, isolated by SEC in an apparent dimer↔monomer equilibrium (Fig. 2), both form aggregates when MBP is cleaved off by factor Xa (Fig. 3). The aggregation of the MBP-free hPAH-RDs is prevented by L-Phe (> 95%) for both forms (Fig. 5), and the effect is stereospecific (Fig. 4a). Half-maximal inhibition ($[L]_{0.5}$) was obtained at 23.3 ± 0.5 μM L-Phe (cleaved dimeric fraction) and 15.1 ± 2.4 μM L-Phe (cleaved monomeric fraction). These numbers for the apparent affinity of L-Phe binding to human RD are in good agreement with the K_d-value of 15.2 ± 1.1 μM (n = 0.9 ± 0.1 sites per monomer) measured for the rat RD dimer by ITC [8]). In both the rat and human dimeric forms, a positive cooperativity of L-Phe binding was observed, with a calculated Hill coefficient (n_H) value of ~ 2.

That L-Phe also binds to the MBP-hPAH-RD dimer before factor Xa cleavage was shown by its reduction of the ANS fluorescence enhancement observed upon the binding of the hydrophobic fluorescence probe to the fusion protein (Fig. 6A). Also, in this assay system, the measured responses to L-Phe were stereospecific (Figs 4A and 6A), with L-Phe being present in a physiological concentration range (Fig. 6). This finding indicates that the dimer formation of the fusion protein is based on an interaction between the RDs of two protomers, capable of binding L-Phe.

In contrast to wt-MBP-hPAH-RD, a structurally/conformationally variant mutant form (MBP-hPAH-G46S-RD, Fig. 1A) revealed no protection against aggregation by L-Phe upon cleavage by factor Xa of its dimeric form. The lack of stabilizing effect indicates that the binding site in the RD is sensitive to the conformation of its $\beta_1\alpha_1\beta_2\beta_3\alpha_2\beta_4$ sandwich fold. In the crystal structure of the hPAH-RD [16] L-Phe binding includes the sequence region E^{43}xVxAL in the two protomers. The residue G46 is positioned at the entry of α-helix 1 (A^{47}-E^{57}) in a five residue (L^{41}-G^{46}) loop structure (loop 1), linking β-strand 1 and α-helix 1.

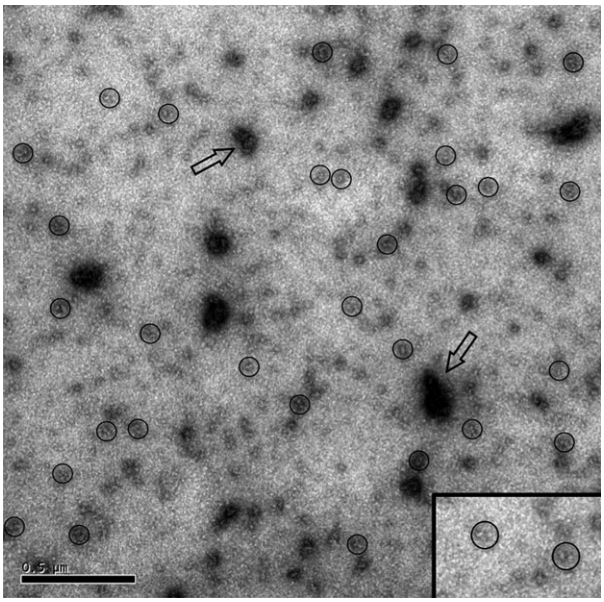

Fig. 7. Electron micrograph of MBP-free wt-hPAH-RD$^{1–120}$ [complete cleavage of its MBP fusion protein by factor Xa (t = 3 h)]. The proteins were negatively stained with aqueous uranyl acetate and imaged in the JEOL 1230 Transmission Electron Microscope operated at 80 kV. Structures with a dimeric appearence, corresponding to about 20% of the small-sized structures are circled and also highlighted in the inset. The open arrows indicate larger protein aggregates. Scale bar: 500 nm.

The substitution G46→S is predicted to promote a N-terminal extension of α-helix 1 by four residues, or one turn [20].

In conclusion, we report a method for the preparation of highly pure, metastable and soluble dimeric↔monomeric forms of the human N-terminal RD as a MBP fusion protein. Our data support previous biochemical and biophysical studies on isolated recombinant rat and human RDs, that is: (i) L-Phe binds to a recombinant RD dimer in a physiological concentration range and stabilizes the structure; and (ii) L-Phe binds with relatively high affinity and with a positive cooperativity (n_H about 2). In addition, our data demonstrate that the binding is stereospecific for L-Phe, and that the RD mutation G46S prevents the binding of L-Phe and its protection against aggregation of MBP-free RD. This effect is explained by a structural/conformational change in its wt-binding site involving the residues E^{43}xVxAL in dimeric $\beta_1\alpha_1\beta_2\beta_3\alpha_2\beta_4$ ACT domain folds. Overall, our data are compatible with an emerging model of the full-length PAH in which L-Phe binding to dimerized RDs may be involved in the complex substrate activation process of this multidomain enzyme. However, in contrast to the catalytic domain [13] there is no crystal structure available for the substrate-bound form of the homotetramer [8,15].

Acknowledgements

This work was supported by Fundação para a Ciência e a Tecnologia, Portugal, grant SFRH/BD/19024/2004 and the University of Bergen, Norway. We are indebted to Professor Aurora Martínez for helpful comments and discussions.

Author contributions

JL and TF designed the study; JL, JS and TF analysed the data and wrote the manuscript. All authors have read and approved the manuscript.

References

1 Fitzpatrick PF (2015) Structural insights into the regulation of aromatic amino acid hydroxylation. *Curr Opin Struct Biol* **35**, 1–6.
2 Frieden C (1970) Kinetic aspectes of rregulation of metabolic protesses. The hysteretic enzyme concept. *J Biol Chem* **245**, 5788–5799.
3 Shiman R and Gray DW (1980) Substrate activation of phenylalanine hydroxylase. A kinetic characterization. *J Biol Chem* **255**, 4793–4800.
4 Kobe B, Jennings IG, House CM, Michell BJ, Goodwill KE, Santarsiero BD, Stevens RC, Cotton RG and Kemp BE (1999) Structural basis of autoregulation of phenylalanine hydroxylase. *Nat Struct Biol* **6**, 442–448.
5 Zhang S, Roberts KM and Fitzpatrick PF (2014) Phenylalanine binding is linked to dimerization of the regulatory domain of phenylalanine hydroxylase. *Biochemistry* **53**, 6625–6627.
6 Roberts KM, Kahn CA, Hinck CS and Fitzpatrick PF (2014) Activation of phenylalanine hydroxylase by phenylalanine does not require binding in the active site. *Biochemistry* **53**, 7846–7853.
7 Zhang S and Fitzpatrick PF (2016) Identification of the allosteric site for phenylalanine in rat phenylalanine hydroxylase. *J Biol Chem* **291**, 7418–7425.
8 Meisburger SP, Taylor AB, Khan CA, Zhang S, Fitzpatrick PF and Ando N (2016) Domain movements upon activation of phenylalanine hydroxylase characterized by crystallography and chromatography-coupled small-angle X-ray scattering. *J Am Chem Soc* **138**, 6506–6516.
9 Martínez A, Haavik J and Flatmark T (1990) Cooperative homotropic interaction of L-noradrenaline with the catalytic site of phenylalanine 4-monooxygenase. *Eur J Biochem* **193**, 211–219.
10 Martínez A, Olafsdottir S and Flatmark T (1993) The cooperative binding of phenylalanine to phenylalanine 4-monooxygenase studied by ^{1}NMR paramagnetic relaxation. Changes in water accessibility to the iron at the active site upon substrate binding. *Eur J Biochem* **211**, 259–266.
11 Thórólfsson M, Ibarra-Molero B, Fojan P, Petersen SB, Sanchez-Ruiz JM and Martínez A (2002) L-Phenylalanine binding and domain organization in human phenylalanine hydroxylase: a differential scanning calorimetry study. *Biochemistry* **41**, 7573–7585.
12 Thórólfsson M, Teigen K and Martínez A (2003) Activation of phenylalanine hydroxylase: effect of substitutions at Arg68 and Cys237. *Biochemistry* **42**, 3419–3428.
13 Andersen OA, Stokka AJ, Flatmark T and Hough E (2003) 2.0 Å resolution crystal structures of the ternary complexes of human phenylalanine hydroxylase catalytic domain with tetrahydrobiopterin and 3-(2-thienyl)-L-alanine or L-norleucine: substrate specificity and molecular motions related to substrate binding. *J Mol Biol* **333**, 747–757.
14 Flydal MI, Mohn TC, Pey AL, Siltberg-Liberles J, Teigen K and Martínez A (2010) Superstoichiometric binding of L-Phe to phenylalanine hydroxylase from *Caenorhabditis elegans*: evolutionary implications. *Amino Acids* **39**, 1463–1475.
15 Arturo EC, Gupta K, Heroux A, Stith L, Cross PJ, Parker EJ, Loll PJ and Jaffe EK (2016) First structure of full-length mammalian phenylalanine hydroxylase

reveals the architecture of an autoinhibited tetramer. *Proc Natl Acad Sci U S A* **113**, 2394–2399.
16 Patel D, Kopec J, Fitzpatrick F, McCorvie TJ and Yue WW (2016) Structural basis for ligand-dependent dimerization of phenylalanine hydroxylase regulatory domain. *Sci Rep* **6**, 23748.
17 Eiken HG, Knappskog PM, Apold J and Flatmark T (1996) PKU mutation pG46S is associated with increased aggregation and degradation of the phenylalanine hydroxylase enzyme. *Hum Mutat* **7**, 228–238.
18 Martínez A, Knappskog PM, Olafsdottir S, Døskeland AP, Eiken HG, Svebak RM, Bozzini M, Apold J and Flatmark T (1995) Expression of recombinant human phenylalanine hydroxylase as fusion protein in *Escherichia coli* circumvents proteolytic degradation by host cell proteases. Isolation and characterization of the wild-type enzyme. *Biochem J* **306**, 589–597.
19 Bradford MM (1976) A rapid and sensitive method for the quantitation of microgram quantities of protein utilizing the principle of protein-dye binding. *Anal Biochem* **72**, 248–254.
20 Leandro J, Simonsen N, Saraste J, Leandro P and Flatmark T (2011) Phenylketonuria as a protein misfolding disease: the mutation pG46S in phenylalanine hydroxylase promotes self-association and fibril formation. *Biochim Biophys Acta* **1812**, 106–120.
21 Kang GJ, Cooney DA, Moyer JD, Kelley JA, Kim H-Y, Marquez VE and Johns DG (1989) Cyclopentenylcytosine triphosphate. Formation and inhibition of CTP synhetase. *J Biol Chem* **264**, 713–718.
22 Laemmli UK (1970) Cleavage of structural proteins during the assembly of the head of bacteriophage T4. *Nature* **227**, 680–685.
23 Aukrust I, Evensen L, Hollås H, Berven F, Atkinson RA, Trave G, Flatmark T and Vedeler A (2006) Engineering, biophysical characterization and binding properties of a soluble mutant form of annexin A2 domain IV that adopts a partially folded conformation. *J Mol Biol* **363**, 469–481.
24 Semisotnov GV, Rodionova NA, Razgulyaev OI, Uversky VN, Gripas AF and Gilmanshin RI (1991) Study of the "molten globule" intermediate state in protein folding by a hydrophobic fluorescent probe. *Biopolymers* **31**, 119–128.
25 Kapust RB and Waugh DS (1999) *Escherichia coli* maltose-binding protein is uncommonly effective at promoting the solubility of polypeptides to which it is fused. *Protein Sci* **8**, 1668–1674.
26 Kabsch W and Sander C (1983) Directory of protein secondary structure: pattern recognition of hydrogen-bonded and geometrical features. *Biopolymers* **22**, 2577–2637.
27 DeLano SL (2002) *The PyMOL Molecular Graphics System*. DeLano Scientific LLC, South San Francisco, CA.